Accumulation effect of SiO_2 protective layer on multi-shot laser-induced damage in high-reflectivity HfO_2 /SiO_2 coatings

Ying Wang (王 营)[1,2*], Hongbo He (贺洪波)[1], Yuan'an Zhao (赵元安)[1], Yongguang Shan (单永光)[1,2], Chaoyang Wei (魏朝阳)[1]

[1]*Key Laboratory of Materials for High Power Lasers, Shanghai Institute of Optics and Fine Mechanics, Chinese Academy of Sciences, Shanghai 201800, China*

[2]*Graduate University of Chinese Academy of Sciences, Beijing 100049, China*

[*]*Corresponding author: wangying@siem.ae.cn*

Received February 14, 2011; accepted May 9, 2011; posted online August 5, 2011

The accumulation effects in high-reflectivity (HR) HfO_2/SiO_2 coatings under laser irradiation are investigated. The HR HfO_2/SiO_2 coatings are prepared by electron beam evaporation at 1 064 nm. The laser-induced damage threshold (LIDT) are measured at 1 064 nm and at a pulse duration of 12 ns, in 1-on-1 and S-on-1 modes. Multi-shot LIDT is lower than single-shot LIDT. The laser-induced and native defects play an important role in the multi-shot mode. A correlative theory model based on critical conduction band electron density is constructed to elucidate the experimental phenomena.

OCIS codes: 310.0310, 140.3330.

doi: 10.3788/COL201109.103103.

In recent years, many laboratories have investigated multi-shot laser-induced damage in optical materials, such as fused silica[1] and KTP crystals[2]. The multi-shot laser-induced damage threshold (LIDT) is often lower than single-shot LIDT because of the accumulation effects in most optical materials[1,3−5]. As a result, investigations on multi-shot laser-induced damage in optical coatings are of high practical importance for high-power laser applications[5,6]. The mechanism for single-shot laser damage includes avalanche ionization (AI)[7], multiphoton ionization (MPI)[8], impurity breakdown[9], etc. However, the damage mechanism of multi-shot radiation is considerably more complicated than that of single-shot radiation. Mero *et al.* established a model for studying multi-shot damage behavior in the femtosecond regime[6]. In another previous study, a model was developed to explain the correlations between observed multi-shot laser damage threshold and its dependence on the number of shots in the nanosecond regime[10]. The aim of this letter is to identify the correlations between observed LIDT and the characteristics of the native and laser-induced defects in multilayers under single- and multi-shot radiation. We present the results of 1-on-1 and S-on-1 tests at 1 064 nm for high-reflectivity (HR) HfO_2/SiO_2 coatings. Then, we provide the experimental details of the sample deposition process and laser damage test procedure. Finally, the experimental results and discussions are presented.

The samples were prepared by electron beam evaporation. The coating design of the sample was G|$(HL)^{13}$H4L|A, where H denotes the high-index HfO_2 with one quarter wavelength optical thickness (QWOT), L is the low-index SiO_2 with one QWOT, G represents the BK7 substrate, and A is the incident medium (air). The transmittance spectra of the sample are shown in Fig. 1.

The experimental setup for laser damage is schematically shown in Fig. 2[5]. The Nd:YAG laser system was operated in TEM_{00} mode and the pulse width was 12 ns at 1 064 nm. The beams were focused onto a $1/e^2$ height of 320 μm and width of 250 μm. In the S-on-1 test, the sample was tested at a frequency of 5 Hz. The laser energy used to damage the sample was obtained by adjusting the attenuator, and the pulse energy was measured by using an energy meter from a split-off portion of the beam. The sample was set on a two-dimensional precision stage driven by a stepper motor. The He-Ne laser was used to monitor the test. Damage onset was detected on-line using a video microscopy system.

The S-on-1 test was carried out in accordance with the ISO 11254-2 standard[11]. In this letter, 1, 5, 10, 20, 100, and 1 000-on-1 LIDT were tested to understand the influence of the number of laser shots N on the accumulation effects. Twenty sites were tested at each selected fluence for 1-on-1, and 10 sites were chosen for S-on-1.

Laser damage threshold was determined by linear

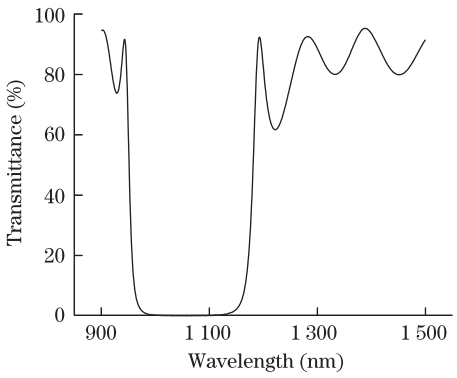

Fig. 1. Transmittance spectra of the sample.

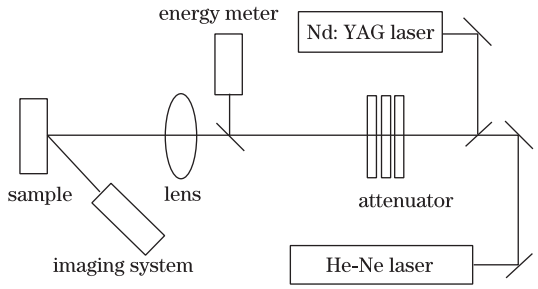

Fig. 2. Experimental setup of the laser damage test.

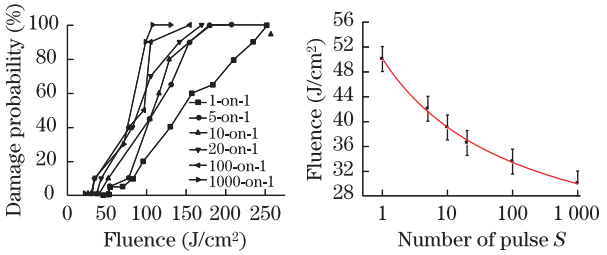

Fig. 3. (a) S-on-1 damage probability curves and (b) LIDT as a function of pulse number S, fit according to Eq. (1).

extrapolation of the damage probability data to zero damage probability, in accordance with the ISO11254-1, -2 standards[11,12]. Two representations of the damage probability data are shown in Fig. 3. The S-on-1 damage probability curves with S ranging from 1 to 1000 are shown in Fig. 3(a). The 0% damage probability is depicted in Fig. 3(b). The accumulation effects are clarified in the two representations.

The data in Fig. 3(a) show that the damage probability increases with increasing pulse number. The slope of the damage probability appears sharper when the shot number increases. This result indicates that the creation of laser-induced defects is related to multi-shot damage. Generating laser-induced defects under multi-shots is possible. Figure 3(b) shows that the 0% damage probability drops dramatically after the first several laser shots, until it reaches a constant level.

The damage morphology of the HR coatings was mapped using a Leica optical microscope and WYKO surface profiler. The damage morphology and depth information are shown in Fig. 4. Morphology observation enables views of damage characteristics. The damages originate from the defects as reflected in both the 1-on-1 and S-on-1 tests (Fig. 4). The surrounding defects are plasma scalds resulted from the presence of plasma during the damage process.

Because of the interference effects in the film, local intensity enhancements exist in the sample coatings. The theoretical results for the electric field distributions of the sample were calculated using a thin film design software (TFCalc) and were shown in Fig. 5.

The depth of the damage spot is about 200 nm, corresponding to the peak electric field in the SiO_2 protective layer.

The ISO 11254-2 standard[11] describes a formula that allows for extrapolation of the S-on-1 damage threshold $F_{\rm th}$ for large number N of pulses. The extrapolation model is based on three fit parameters $F_{\rm th,1}$, $F_{\rm th,\infty}$ and Δ, which can be interpreted as the characteristic parameters of damage behavior:

$$F_{\rm th}(N) = F_{\rm th,\infty} + \frac{F_{\rm th,1} - F_{\rm th,\infty}}{1 + \frac{1}{\Delta}\log_{10} N} + d, \qquad (1)$$

where $F_{\rm th,1}$ describes the 1-on-1 damage threshold; $F_{\rm th,\infty}$ can be considered the endurance limit of the optical surface; Δ is given by the intersection of the tangent at point $(1,F_{\rm th,1})$ and constant level $F_{\rm th,\infty}$ and it describes the decrease in the characteristic damage curve with the number of pulses. The three parameters ($F_{\rm th,1}$, $F_{\rm th,\infty}$, and Δ) are calculated by a least square fit routine keeping constant d equal to zero. Constant d represents a displacement of the characteristic curve toward smaller damage thresholds to delineate the safe operational limits of the specimen. The result of the extrapolation of the S-on-1 damage threshold is shown in Fig. 7.

Material damage can be explained by the excitation of electrons from the valence band (VB) to the conduction band (CB) via processes such as AI and photo-ionization (PI)[8]. When the electron density (ED) in the CB reaches a critical ED $n_{\rm cr}$ generally considered a damage criterion, the materials absorb strongly through the process of inverse bremsstrahlung resulting in reversible or irreversible changes, represented by[13]

$$n_{\rm cr} = \frac{\varepsilon_0 m^* w^2}{e^2}, \qquad (2)$$

where m^* is the effective conductivity masses of electrons, w is the incident laser frequency , and e denotes the electron charge.

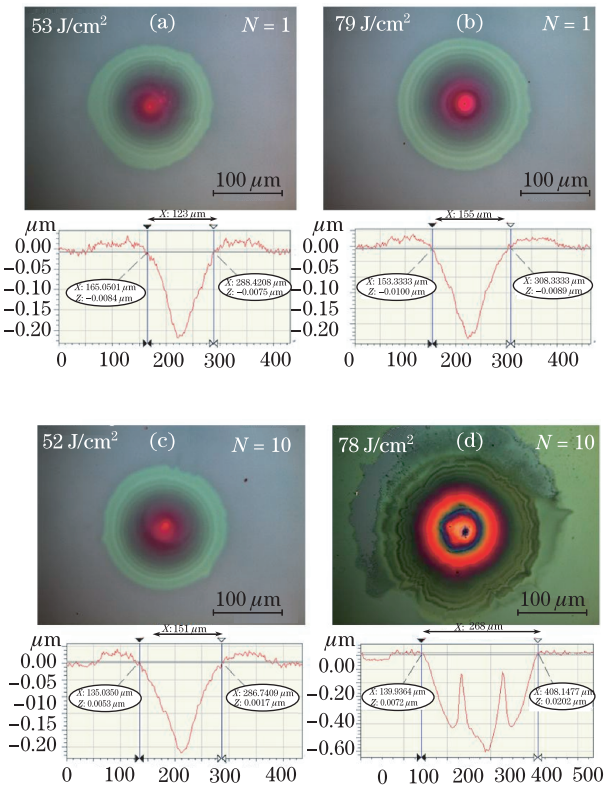

Fig. 4. Damage morphologies and depth information of the HR coatings (a) single shot, F=53 J/cm^2, (b) single shot, F=79 J/cm^2, (c) N=10 laser shots, F=52 J/cm^2, and (d) N=10 laser shots, F=78 J/cm^2.

The absorbing defects often play an important role in nanosecond damage at low frequency[5]. The damages frequently originate from the defects in our experiment (see Fig. 4). To explain the accumulation effects in the wide-gap HfO_2/SiO_2 coatings, the native and laser-induced defects were considered as trapping states[14,15]. The native defects result from thin film deposition procedures, such as vacancy and interstitial ion. The laser-induced defects can be produced by laser irradiation. In our calculation, multiphoton and impact ionization produce only seed electrons, and then these seed electrons achieve critical plasma density through the native absorbing defects. The simplest energy diagram and processes of the model are illustrated in Fig. 6. Once reaching the CB, electrons can relax to the VB with a characteristic time constant $T_{\rm cv}$. The defect trapping rate of electrons from the CB is characterized by a time constant $T_{\rm cl}$.

The ED in the CB is described by the following set of rate equations[16]:

$$\frac{{\rm d}n}{{\rm d}t} = W_{\rm AV}n(t) + W_{\rm PI} + \sigma_{\rm nd}n(t)I(t) - \frac{n(t)}{T_{\rm cv}} + \sigma_{\rm ld}n_{\rm ld}(t)I(t) - \frac{n(t)}{T_{\rm cl}}(1 - \frac{n_{\rm ld}(t)}{n_{\rm ld,max}}), \quad (3)$$

where $W_{\rm AV}$ and $W_{\rm PI}$ are the AI and PI rates, respectively, $\sigma_{\rm nd}$ is the absorption cross-section of the native defects, $n_{\rm ld}$ denotes the number densities of the laser-induced defects, $n_{\rm ld,max}$ represents the maximum density of the laser-induced defects, and $\sigma_{\rm ld}$ is the absorption cross-section of the laser-induced defects. AI rate $W_{\rm AV}$

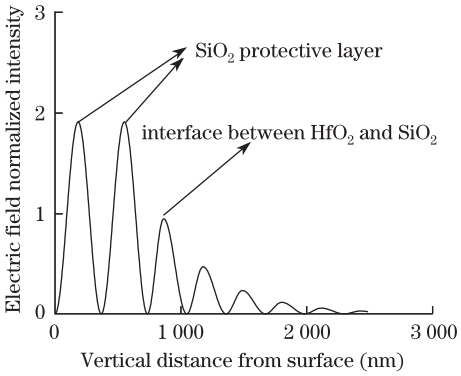

Fig. 5. Electric field intensity profile in HR HfO_2/SiO_2 coatings normalized to the incident electric field value at a wavelength of 1 064 nm.

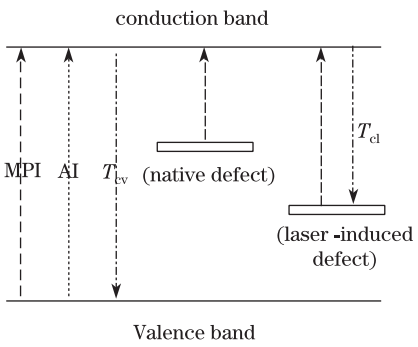

Fig. 6. Diagram of energy levels and transitions in the wide-gap dielectric materials.

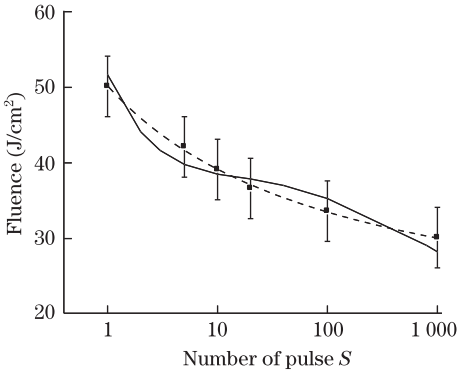

Fig. 7. Multi-shot damage threshold as a function of the number of pulses. The dashed line is a fitting curve according to Eq. (1). The solid lines are simulations from the model based on Eqs. (3)–(6).

is calculated using the Drude model[13] thus:

$$W_{\rm AV} = \frac{\sigma}{E_{\rm g}}I(t), \quad (4)$$

where $\sigma = \frac{e^2}{c\varepsilon_0 n_0 m^*} \bullet \frac{\tau_{\rm c}}{1+w^2\tau_{\rm c}^2}$ is the absorption cross-section, $\tau_{\rm c} = \frac{16\pi\varepsilon_0^2\sqrt{m^*(0.1E_{\rm g})^3}}{\sqrt{2}e^4 n(t)}$ is the resultant collision time, which is reciprocal to the electron density, and $E_{\rm g}$ is the intrinsic material gap. $I(t)$ is the laser intensity, given by $I(t) = I_0\exp[-4\ln(2t^2/\tau^2)]$, where I_0 is the laser fluence and τ is the pulse duration. For low electric fields, the PI rate describes the probability for MPI, and the PI rate can be described by the Keldysh's PI rate theory, which is most commonly used to calculate the excitation rate of electrons[17]:

$$W_{\rm multpt} = \frac{2w}{9\pi}(\frac{m^*w}{\hbar})^3/2\Phi\sqrt{2}\langle E_{\rm g}'/\hbar w\rangle - 2E_{\rm g}'/\hbar w) \times \exp\left[2\langle E_{\rm g}'/\hbar w\rangle\left(1 - \frac{1}{4\gamma^2}\right)\right]\left(\frac{1}{16\gamma^2}\right)^{\langle E_{\rm g}'/\hbar w+1\rangle}. \quad (5)$$

where $\gamma = w\sqrt{m_{\rm e}^* E_{\rm g}}/eE$, E is the electric field oscillating at frequency w, $E_{\rm g}' = E_{\rm g}\left[1 + (1/2\gamma^2)\right]$ represents the effective band gap energy in the radiation field, $m^* = m_{\rm e}m_{\rm h}/(m_{\rm e} + m_{\rm h})$ indicates the reduced effective mass of the conduction electron and valence hole, $m_{\rm h}$ denotes the effective conductivity masses of holes, the symbol $\langle\cdots\rangle$ denotes the integer part, and Φ describes the Dawson function.

The ED in the laser-induced defects is given by

$$\frac{{\rm d}n_{\rm ld}}{{\rm d}t} = \frac{n(t)}{T_{\rm cl}}\left(1 - \frac{n_{\rm ld}(t)}{n_{\rm ld,max}}\right) - \sigma_{\rm ld}n_{\rm ld}(t)I(t). \quad (6)$$

The laser intensity is zero between the pulses. When the CB ED surpasses a critical plasma density $n_{\rm cr}$, the damage occurs. The values of $n_{\rm ld,max}$, $\sigma_{\rm nd}$, and $\sigma_{\rm ld}$ were taken from best fits to experiments.

The band gaps of bulk materials SiO_2 and HfO_2 are 8.3 and 5.1 eV[18], respectively. The damage occurs in the SiO_2 protective layer first, so that the parameters of SiO_2 were used in our calculation. The values for all the parameters in Eqs. (2)–(7) are shown in Table 1. The values for $E_{\rm g}$ are obtained form Ref. [18]. The

Table 1. List of Parameters for HfO_2 and SiO_2

	E_g(eV)	n_0	m^*	m_e=m_h
HfO_2	5.6	1.93	0.635	1.0
SiO_2	7.8	1.43	0.635	1.0

values for m^*, m_e, and m_h are obtained form Ref. [19]. The equations are solved numerically and the values are taken from best fits to experiments from the samples. The simulation result is shown in Fig. 7.

The optical of the material at a certain laser radiation can be varied, causing a laser-induced defect, which in turn lowers the LIDT. The laser-induced defect can be reversible or irreversible. When the irreversible laser-induced defects represent an accumulation effect, the laser fluence below the single-shot LIDT can lead to the damage in the multi-shot procedure. Figure 7 shows that the model can explain the most important features of the experimental data. The LIDT decreases with increasing pulse number and saturates at a certain value.

The above analysis shows that the larger the absorption of native defects, the lower the single-shot damage threshold. Multi-shot laser damage is related to the laser-induced and native defects in the multilayer. The accumulation of irreversible changes in the laser-induced defects results in a multi-shot LIDT lower than that in the single-shot LIDT.

In conclusion, the LIDT exhibits a dependence on laser shot number in multi-shot damage behavior. Accumulation effects are experimentally and theoretically investigated in HR HfO_2/SiO_2 coatings. The decrease in the damage threshold is attributed to the accumulation of irreversible changes in the laser-induced and native defects. A rate equation model for the CB ED via multiphoton and AI is developed to explain the multi-shot damage behavior.

References

1. J. Y. Natoli, B. Bertussi, and M. Commandre, Opt. Lett. **30,** 1315 (2005).
2. F. R. Wagner, A. Hildenbrand, L. Gallais, H. Akhouayri, M. Commandre, and J. Y. Natoli, Proc. SPIE **7132,** 71320Y (2008).
3. S. C. Jones, P. Braunlich, R. T. Casper, X. A. Shen, and P. Kelly, Opt. Eng. **28,** 1039 (1989).
4. A. A. Manenkov and V. S. Nechitailo, Proc. SPIE **1441,** 392 (1991).
5. Y. Zhao, W. Gao, J. Shao, and Z. Fan, Appl. Surf. Sci. **227,** 275 (2004).
6. M. Mero, B. Clapp, J. C. Jasapara, W. Rudolph, D. Ristau, K. Starke, J. Kruger, S. Martin, and W. Kautek, Opt. Eng. **44,** 051107 (2005).
7. A. S. Epifanov, IEEE J. Quantum Electron. **17,** 2018 (1981).
8. N. Bloembergen, IEEE J. Quantum Electron. **10,** 375 (1974).
9. R. W. Hopper and D. R. Uhlmann, J. Appl. Phys. **41,** 4023 (1970).
10. Y. Wang, H. He, Y. Zhao, Y. Shan, D. Li, and C. Wei, Chin. Opt. Lett. **9,** 023103 (2011).
11. ISO11254-2, "Lasers and laser-related equipment-determination of laser-induced damage threshold of optical surfaces-Part 2," in *s-on*-1 test (2000).
12. ISO11254-1, "Lasers and laser-related equipment-determination of laser-induced damage threshold of optical surfaces-Part 1," in 1-*on*-1 test (2000).
13. K. Starke, D. Ristau, H. Welling, T. V. Amotchkina, M. Trubetskov, A. A. Tikhonravov, and A. S. Chirkin, Proc. SPIE **5273,** 501 (2004).
14. L. A. Emmert, M. Mero, and W. Rudolph, J. Appl. Phys. **108,** 043523 (2010).
15. M. Mero, L. A. Emmert, and W. Rudolph, Proc. SPIE **7132,** 713209 (2008).
16. Y. Wang, Y. Zhao, Y. Shan, J. Shao, and Z. Fan, Chin. Opt. Lett. **9,** 093102 (2011).
17. L. V. Keldysh, Sov. Phys. JETP **20,** 1307 (1965).
18. L. Yuan, Y. Zhao, C. Wang, H. He, Z. Fan, and J. Shao, Appl. Surf. Sci. **253,** 3450 (2007).
19. L. Sudrie, A. Couairon, M. Franco, B. Lamouroux, B. Prade, S. Tzortzakis, and A. Mysyrowicz, Phys. Rev. Lett. **89,** 186601 (2002).